



LAWRENCE
LIVERMORE
NATIONAL
LABORATORY

Modeling of Laser-Induced Metal Combustion

C. D. Boley, A. M. Rubenchik

February 29, 2008

5th Annual High Energy Laser Lethality Conference
Monterey, CA, United States
March 3, 2008 through March 7, 2008

Disclaimer

This document was prepared as an account of work sponsored by an agency of the United States government. Neither the United States government nor Lawrence Livermore National Security, LLC, nor any of their employees makes any warranty, expressed or implied, or assumes any legal liability or responsibility for the accuracy, completeness, or usefulness of any information, apparatus, product, or process disclosed, or represents that its use would not infringe privately owned rights. Reference herein to any specific commercial product, process, or service by trade name, trademark, manufacturer, or otherwise does not necessarily constitute or imply its endorsement, recommendation, or favoring by the United States government or Lawrence Livermore National Security, LLC. The views and opinions of authors expressed herein do not necessarily state or reflect those of the United States government or Lawrence Livermore National Security, LLC, and shall not be used for advertising or product endorsement purposes.

Modeling of Laser-Induced Metal Combustion *

C. D. Boley¹ and A. M. Rubenchik²
Lawrence Livermore National Laboratory
Livermore, CA 94551

Experiments involving the interaction of a high-power laser beam with metal targets demonstrate that combustion plays an important role. This process depends on reactions within an oxide layer, together with oxygenation and removal of this layer by the wind. We present an analytical model of laser-induced combustion. The model predicts the threshold for initiation of combustion, the growth of the combustion layer with time, and the threshold for self-supported combustion. Solutions are compared with detailed numerical modeling as benchmarked by laboratory experiments.

Keywords: solid-state laser, high average power, lethality, combustion, analytical model

Nomenclature

a	spot radius
C	specific heat
D	thermal diffusivity
I	laser intensity
Q	combustion power flux
T	temperature
T_c	combustion initiation temperature
α	optical absorptivity
κ	thermal conductivity
ρ	density

1. Introduction

During the last decade, our laboratory at LLNL has been developing solid-state lasers with high average power, for applications to tactical defense. Our most current laser contains four diode-pumped ceramic Nd:YAG slabs¹²⁻¹⁵. It produces approximately 25 kW of average power for 10 seconds, at a wavelength of 1.053 μm . Upon addition of another slab and an

*Work performed under the auspices of the U.S. Department of Energy by Lawrence Livermore National Laboratory under Contract DE-AC52-07NA27344.

¹E-mail address: boley1@llnl.gov; telephone: (925) 423-7365; fax: (925) 423-6195.

²E-mail address: rubenchik1@llnl.gov; telephone: (925) 422-6131.

increased diode duty factor, the laser has yielded 67 kW for 0.25 s. The waveform consists of pulses of length 0.5 ms, at 200 Hz, corresponding to a duty factor of 10%. During lasing operations, waste heat is stored in the slabs. In actual applications, the hot slabs would be rapidly cycled out of the aperture and cooled, while cold slabs would simultaneously be cycled into the aperture.

We have studied the material interactions produced by such lasers, including high-explosive initiation, in some detail¹⁻⁹. Because the thermal conduction length between pulses is small compared to typical target dimensions, the macroscopic heat distribution is generally determined by the time-average power rather than the instantaneous power. At a 10% duty factor, the latter is of course 10 times the former. We have constructed a computational model (THALES²⁻⁹) which yields detailed predictions. At a power near 100 kW, the laser has been projected to be effective in defense against mortars and rockets^{2,8,9}. A lower power suffices for neutralization of threats such as landmines¹ and improvised explosive devices.

We have previously shown that combustion plays an important role in facilitating material heating^{2,3,8}. We have incorporated a model of combustion into THALES and found parameter values which seem consistent with experiment. While this detailed treatment is useful, it does not readily illuminate some general features and trends. Among these are the threshold for combustion and the possibility of self-supported combustion. The latter occurs when combustion reactions continue after the laser has been turned off. This has been observed in LLNL experiments on titanium³ but not on iron^{2,3,8}. An analytical approach can add to our understanding of such issues.

In this paper, we present an analytical model of laser-induced combustion in metals. The model is based on the phenomenology of combustion¹¹, together with solutions of the heat

conduction equation in solids¹⁰. It predicts the threshold for initiation of the combustion process, the relative role of laser heating and energy deposition due to combustion affects, and the threshold for self-supported combustion. We compare analytical results with evidence from experiments. The model appears to be consistent with this evidence.

2. Model

The equation governing heat conduction within a solid is

$$\rho C \frac{\partial T}{\partial t} = \kappa \nabla^2 T, \quad (1)$$

where T is the local temperature, ρC is the heat capacity per volume, and κ is the thermal conductivity. We shall also use $D = \kappa / \rho C$, the thermal diffusivity. We assume that the material properties can be treated as constants. We work in cylindrical coordinates (z, r) , so that the temperature has the dependence $T(z, r, t)$. Energy is supplied to the system by both laser heating and combustion. We assume that the beam is turned on at $t = 0$ and thereafter is constant. The intensity distribution is taken to be Gaussian. Thus the absorbed laser flux has the form

$$P(r) = \alpha I_0 \exp(-r^2 / a^2), \quad (2)$$

where α is the surface absorptivity and a is the spot radius.

Combustion occurs within a thin oxide layer on the surface¹¹. The combustion products are rapidly removed by the wind. Making simple assumptions regarding the turbulent boundary layer³, one finds that the energy flux due to combustion takes the form

$$Q = Q_c \exp(-T_c / T), \quad (3)$$

with Q_c proportional to the wind speed. Modeling the laser irradiation of iron at Mach 0.3, we found³ that the temperature response was consistent with $Q_c = 0.8 \text{ kW/cm}^2$ and $T_c = 2000 \text{ K}$. To get a qualitative understanding of the combustion effect, we approximate this flux as a step

function in temperature. We say that the combustion flux equals Q_c for temperatures above a particular “on-off” temperature T_0 , while it vanishes for temperatures below this,

$$Q \approx \begin{cases} Q_c & T > T_0, \\ 0 & T < T_0. \end{cases} \quad (4)$$

The quantity T_0 is of the same order as T_c but the two are not necessarily equal. Under the reasonable assumption that the temperature decreases monotonically away from the center of the beam, the combustion flux is a flat-top with radius $R(t)$, defined by the condition

$T[z = 0, r = R(t), t] = T_0$. For qualitative purposes, we neglect the modification of the surface profile by material removal. This is most appropriate for large spot sizes.

These considerations regarding the energy sources are summarized in the boundary condition:

$$\kappa \left(\frac{\partial T}{\partial z} \right)_{z=0} = P + Q. \quad (5)$$

Thus we have a temperature distribution produced by two sources – a Gaussian function in radius produced by the laser and a step function in radius due to combustion. Since the heat conduction equation is linear, the solution is the sum of the solutions due to each source separately. The solution at the surface will suffice for our purposes.

The temperature distribution due to a given heat flux is a familiar problem for which many explicit solutions are available¹⁰. For our laser source, the surface temperature can be written as

$$T_p(z = 0, r, t) = \frac{\alpha a I_0}{2\pi^{1/2}\kappa_0} \int_0^{\tilde{t}} \frac{dx}{(1+x)x^{1/2}} \exp[-(r/a)^2/(1+x)], \quad (6)$$

where $\tilde{t} = 4Dt/a^2$. Similarly, the surface temperature due to a heat flux Q_0 delivered within a radius r_0 has the form

$$T_Q(z=0, r, t) = \frac{RQ_0}{\kappa} \int_0^\infty J_0(kr) J_1(kr_0) \text{erf}[k(Dt)^{1/2}] \frac{dk}{k}, \quad (7)$$

in terms of Bessel functions and the error function. If r_0 changes slowly in time compared to the average surface temperature, this equation will remain approximately valid. In our model, we assume that this condition is satisfied.

Putting these results together, we see that the combustion radius $R(t)$ is determined by the condition

$$T_0 = T_p[0, R(t), t] + T_Q[0, R(t), t]. \quad (8)$$

It will be convenient to arrange this in the final dimensionless form

$$1 = \tilde{I} \int_0^{\tilde{r}} \frac{dx}{(1+x)x^{1/2}} \exp[-(\tilde{r})^2/(1+x)] + \tilde{q} \tilde{r} \int_0^\infty J_0(\lambda) J_1(\lambda) \text{erf}[\lambda(\tilde{t})^{1/2}/2\tilde{r}] \frac{d\lambda}{\lambda}, \quad (9)$$

where the dimensionless radius of combustion, the dimensionless intensity, and the dimensionless combustion flux are defined by, respectively,

$$\tilde{r} = R(t)/a, \quad \tilde{I} = \alpha a I_0 / 2\pi^{1/2} T_0, \quad \tilde{q} = a Q_c / \kappa T_0. \quad (10)$$

The dimensionless time was defined after Eq. (6). Equation (9) is the basic statement of our model. This is a nonlinear condition giving the radius of combustion as a function of time, for particular values of the laser intensity and combustion flux.

In the regime of interest, the solutions of Eq. (9) have a characteristic behavior. Before a particular time $t_0 > 0$, there is no solution. At this time, there occurs a single solution which develops two branches for larger times. One of these has a radius increasing with time, while the

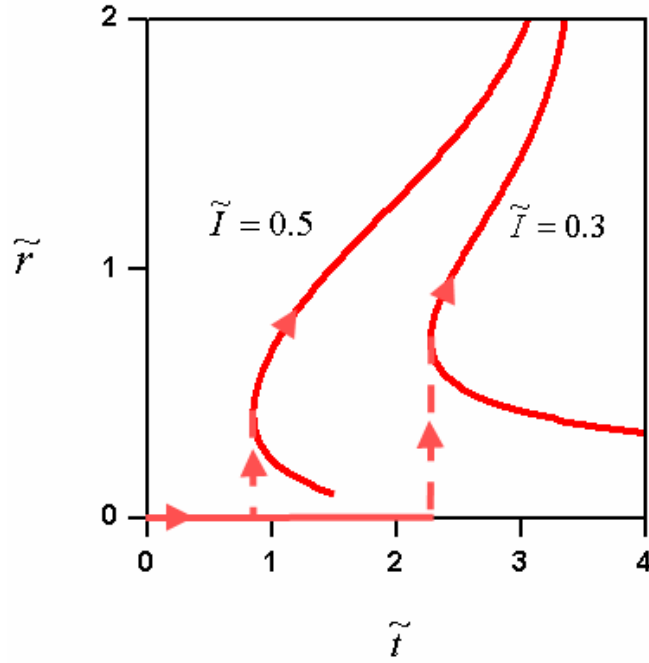


Fig. 1. Evolution of dimensionless combustion radius with dimensionless time, for two choices of the dimensionless intensity \tilde{I} . Here the dimensionless combustion flux is $\tilde{q} = 1.1$.

other has a radius decreasing with time, as illustrated in Fig. 1. Only the former branch is physical. A natural interpretation of this behavior is that, before the threshold time t_0 , the radius is zero. The system then develops an instability which causes the solution to jump to the stable branch. The entire solution follows the arrows shown in Fig. 1. Here two typical solutions, corresponding to two choices of the intensity, are given. As the intensity decreases, the threshold time increases and the curves move to the right.

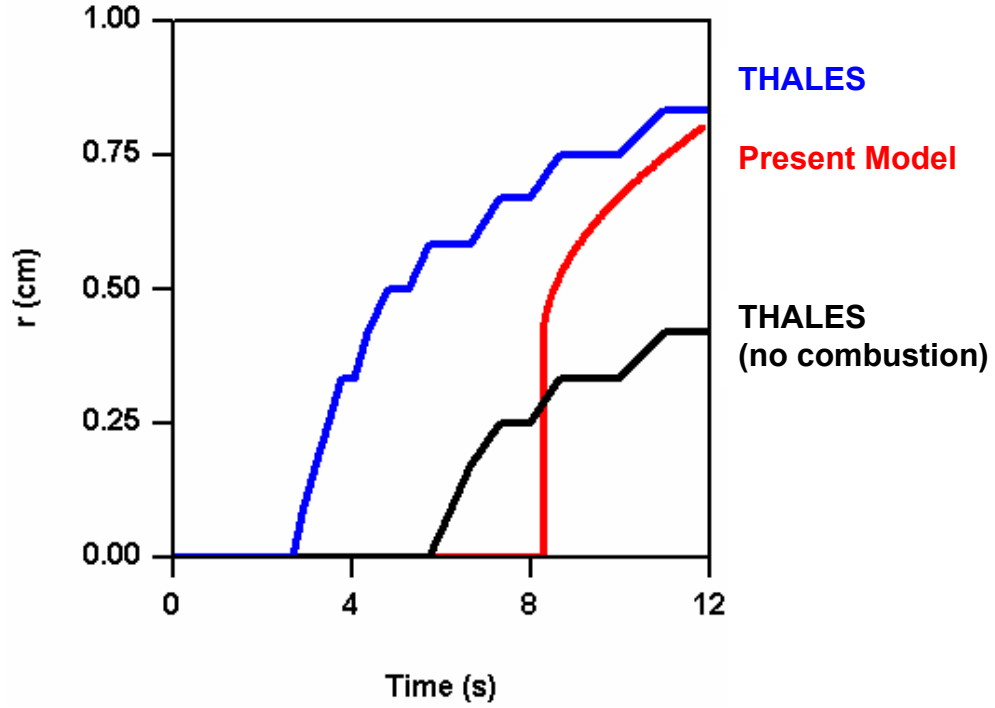


Fig. 2. Evolution of radius with temperature $T_0 = 1400$ C. Red line: Present model; blue line: detailed THALES calculation; black line: THALES calculation without combustion.

3. Applications

We now turn to practical applications, beginning with the laser irradiation of an iron slab. We work with a laser power of 6.3 kW and a spot radius of 1 cm, corresponding to a central intensity of 2 kW/cm^2 . We use $Q_c = 0.8 \text{ kW/cm}^2$, as noted after Eq. (3), and try $T_0 = 1400$ C, remembering that this need not be the same as T_c . The other assumed material parameters are $\rho C = 5.2 \text{ J/(cm}^3 \text{ K)}$, $\kappa = 0.4 \text{ W/(cm K)}$, and $\alpha = 0.5$. These represent reasonable values within the temperature range of interest.

Figure 2 shows the time dependence of the predicted combustion radius, where $T = T_0$. This radius becomes nonzero at a threshold time somewhat greater than 8 s, at which it jumps to

about 0.4 cm and then rises steadily. The figure also shows the corresponding result given by detailed THALES modeling with the combustion flux of Eq. (3) and the same material parameters as above. This indicates a gentler initial rise, as would be expected. The two predictions become comparable at longer times. Finally, the location of this radius is shown for a THALES calculation without combustion. This clearly has a milder behavior than either of the results involving combustion. From these features, we infer that the analytical model is qualitatively realistic.

Next, we turn to the issue of self-supported combustion (ignition). We can obtain a relevant estimate by considering the model, as defined by Eq. (9), in the limit of zero intensity and long time. We have

$$1 = \tilde{q} \tilde{r} \int_0^\infty J_0(\lambda) J_1(\lambda) \frac{d\lambda}{\lambda}, \quad (11)$$

which implies that the (dimensional) radius of combustion is $R = \pi \kappa T_0 / 2 Q_c$. We see that in order for this situation to be reached, the beam radius must be sufficiently large:

$$a \geq \pi \kappa T_0 / 2 Q_c. \quad (12)$$

This is also consistent with dimensional analysis, within a factor of order unity. However, dimensional analysis gives no assurance that ignition will actually occur, in contrast with our model.

We would not expect Eq. (12) to be satisfied in iron, where self-supported combustion was not observed in experiments^{2,3,8}. However, it turns out to be nominally satisfied, since $a = 1.7$ cm (the circular equivalent of the experimental 3x3 cm² beam) and the right-hand side is 1.3 cm. We conjecture that this is due to inaccuracies in our nominal model parameters. It may

be that the experiments would have reached ignition for a somewhat larger spot size, at fixed central intensity and thus greater power.

In titanium, however, the situation is much more definite. The ignition condition (12) is more likely to be satisfied for three reasons: (1) the thermal conductivity is approximately one-third that of iron, depending on the temperature; (2) titanium burns at a much lower temperature than iron (~ 1000 K versus ~ 2000 K); and (3) the heat of combustion is at least comparable to that of iron¹¹. These considerations appear to explain why titanium ignited in our experiments.

4. Conclusions

We have presented an analytical model of laser-induced combustion in metals. The model incorporates simple principles of combustion together with the heat conduction equation. Evaluating solutions of the model, we have found that it predicts a threshold for the combustion process, followed by an increase of the combustion radius with time. It also gives a threshold for self-supported combustion. To the extent that experiments are available in this regime, the model appears to be consistent with reality.

Acknowledgments

We are happy to acknowledge our debt to R. M. Yamamoto, project manager of the LLNL high average power laser program.

References

- ¹Boley, C. D., C. B. Dane, S. N. Fochs, T. J. McGrann, and A. M. Rubenchik, "On Excavation and Destruction of Landmines by a High-Energy Pulsed Laser," Sixth Annual Directed Energy Symposium, Albuquerque, NM, Oct. 20-24, 2003 (UCRL-PRES-153899).
- ²Boley, C. D., S. N. Fochs, and A. M. Rubenchik, "Lethality of a High-Power Solid-State Laser," Ninth Annual Directed Energy Symposium, Albuquerque, NM, Oct. 30 – Nov. 3, 2006 (UCRL-PRES-225460).
- ³Boley, C. D., S. N. Fochs, and A. M. Rubenchik, "Lethality Effects of a High-Power Solid-State Laser," Fourth High Energy Laser Lethality Conference, Monterey, CA, March 19-23, 2007 (UCRL-PRES-228666); UCRL-JRNL-234510, Sept. 11, 2007.
- ⁴Boley, C. D., and A. M. Rubenchik, "Modeling of Material Removal by Solid State Heat Capacity Lasers," Proc. 15th Annual Solid State and Diode Laser Technology Review, Albuquerque, NM, June 3-6, 2002.
- ⁵Boley, C. D., and A. M. Rubenchik, "Modeling of High-Energy Pulsed Laser Interactions with Coupons," University of California, UCRL-ID-151857, Feb. 6, 2003.
- ⁶Boley, C. D., and A. M. Rubenchik, "Simulations of Target Interactions with Pulsed, High-Energy Laser," Proc. 17th Annual Solid State and Diode Laser Technology Review, Albuquerque, NM, June 8-10, 2004.
- ⁷Boley, C. D., and A. M. Rubenchik, "Modeling of the Initiation of High-Explosive Targets by Solid-State Heat Capacity Lasers," Seventh Annual Directed Energy Symposium, Rockville, MD, Oct. 18-21, 2004 (UCRL-PRES-207230).
- ⁸Boley, C. D., and A. M. Rubenchik, "Lethality of High-Power Solid-State Lasers on High-Explosive Targets," Eighth Annual Directed Energy Symposium, Lihue, HI, Nov. 14-18, 2005 (UCRL-PRES-216504).
- ⁹Boley, C. D., and A. M. Rubenchik, "Modeling of Antimortar Lethality by a Solid-State Heat-Capacity Laser," J. Directed Energy **2**, 97-106 (2006).
- ¹⁰Carslaw, H. S., and J. C. Jaeger, "Conduction of Heat in Solids," 2nd Edition, Clarendon Press, Oxford, 1959.
- ¹¹Prokhorov, A. M., V. I. Konov, I. Ursu, and I. N. Mihailescu, "Laser Heating of Metals," Adam Hilger, 1990.
- ¹²Soules, T. F., *et al.*, "Ceramic Nd:YAG – Current Material of Choice for SSHCL," Eighth Annual Directed Energy Symposium, Lihue, HI, Nov. 14-18, 2005.
- ¹³Yamamoto, R. M., *et al.*, "Laser Performance of the Solid-State Heat-Capacity Laser (SSHCL)," Ninth Annual Directed Energy Symposium, Albuquerque, NM, Oct. 30 – Nov. 3, 2006.
- ¹⁴Yamamoto, R. M., *et al.*, "Evolution of a Solid State Laser," Defense and Security Symposium, SPIE, Orlando, FL, April 9-13, 2007 (UCRL-ABS-229142).
- ¹⁵Yamamoto, R. M., *et al.*, "The Use of Large Transparent Ceramics in a High Powered , Diode Pumped Solid State Laser," ASSP 2008, Nara, Japan, Jan. 27-30, 2008 (UCRL-CONF-235413).